

# Compression properties of cellular AlCu5Mn alloy foams with wide range of porosity

Dong-Hui Yang · Shang-Run Yang ·  
Ai-Bin Ma · Jin-Hua Jiang

Received: 17 April 2009 / Accepted: 23 July 2009 / Published online: 6 August 2009  
© Springer Science+Business Media, LLC 2009

**Abstract** Cellular AlCu5Mn foams with porosity of 91.2–45.8% were fabricated by melt-foaming method. The measured compression properties show that both strength and energy absorption capacity of cellular AlCu5Mn foams are better than those of the other Al-based foams. The highest values of strength and energy absorption capacity of cellular AlCu5Mn foams are 82.7 MPa and 72.22 MJ m<sup>-3</sup>, respectively, which implies that cellular AlCu5Mn foams should be attractive in practical applications.

## Introduction

Metallic foam is a class of attractive materials, which exhibits unique combination of physical, mechanical, thermal, electrical, and acoustic properties [1, 2]. In particular, it is light and good at absorbing energy, which is drawing extensive attention in construction, automobile, and aerospace applications from the viewpoint of environmental preservation [2, 3]. Cellular Al/Al alloy foams with relative high porosity (~80%) have been well developed and their mechanical properties as well as their related energy absorption characteristics have been widely studied [4, 5]. With relatively low-energy absorption capacity, which is not more than 13 MJ m<sup>-3</sup> [6, 7], and low strength, which is usually less than 15 MPa [1], the

application of Al foams is limited. The mechanical performance of metallic foams was found to be strongly affected by foam characteristics like porosity, cell size, cell shape, and cell wall strength, etc. Generally, the foams with low porosity, small cell size, and high cell wall strength are supposed to possess better mechanical properties than those with high porosity, big cell size, and low cell wall strength. In recent years, based on the results of revealing relationship between thermal decomposition properties of titanium hydride, the blowing agent, and Al alloy melt foaming process, we have furnished a method to prepare Al alloy foams with relative low porosity (<75%) and small cell size (<1 mm) [8–10]. In this article, we fabricated the cellular AlCu5Mn foams with porosity of 91.2–45.8% by melt-foaming method and investigated their compression and energy absorption properties. Comparing these properties of cellular AlCu5Mn foams with those of other Al-based foams, which possess good mechanical properties and energy absorption capacities [11–14], leads to a conclusion that cellular AlCu5Mn foams should be attractive in practical applications.

## Experimental

An Al alloy containing 4.5–5.3 wt% Cu, 0.6–1.0 wt% Mn, and 0.15–0.35 wt% Ti (AlCu5Mn), which possesses good mechanical properties [15, 16], was used as the matrix material. Ca particles (purity >99.9 wt%) was selected as the thickening agent and the as-received titanium hydride powder (purity >99.2 wt%, Φ 40 μm) was chosen as the blowing agent. The melt-foaming method was applied to prepare the cellular AlCu5Mn foams and the specific fabrication process has been reported in Ref. [10]. Briefly, the thickened Al alloy melt was foamed by adding titanium

D.-H. Yang (✉) · A.-B. Ma · J.-H. Jiang  
College of Materials Science and Engineering,  
HoHai University, Nanjing 210098, China  
e-mail: yang\_donghui76@hotmail.com

S.-R. Yang  
Department of Chemistry, School of Chemistry and Chemical  
Engineering, Nanjing University, Nanjing 210093, China

hydride powder at a proper foaming temperature and the pore structures of the final products were controlled by adjusting the stirring foaming time, holding foaming time, impellor stirring speed as well as selecting the moment the melt foam being initiated to be solidified. As a result, cellular AlCu5Mn foam samples with porosities (Pr) of 91.2–45.8% and cell size ( $D$ ) of  $\sim 3$  to  $\sim 0.5$  mm were obtained.

In this study, the porous Al/Al alloy foams were also fabricated by the melt-infiltration method [17], and parts of porous Al alloy samples were processed by T6 heat treatment to increase the cell wall strength [18]. The starting materials used to prepare the porous Al/Al alloy foams are commercially pure Al, AlSi7 Mg (Si 6.5–7.5 wt%, Mg 0.25–0.45 wt%, Al Bal.), AlSi9Cu2Mg (Si 8.0–10.0 wt%, Cu 1.3–1.8 wt%, Mg 0.4–0.6 wt%, Mn 0.1–0.35 wt%, Ti 0.1–0.35 wt%, Al Bal.), AlCu5MnCdVA (Cu 4.6–5.3 wt%, Mn 0.3–0.5 wt%, Ti 0.15–0.35 wt%, Cd 0.15–0.25 wt%, V 0.05–0.3 wt%, Zr 0.05–0.2 wt%, B 0.005–0.06 wt%, Al Bal.), and AlCu5Mn.

Using fabricated foams, the cylinder compression specimens were made by electro-discharging machine. In order to avoid the cell-size effect on the compression properties of cellular metals[19], the sizes of the specimens are  $\Phi 40$  mm  $\times$  60 mm and  $\Phi 20$  mm  $\times$  30 mm for porosities higher and lower than 80%, respectively. The porosity of a specimen was calculated from its mass ( $M$ ) and volume ( $V_s$ ) using the following expression:

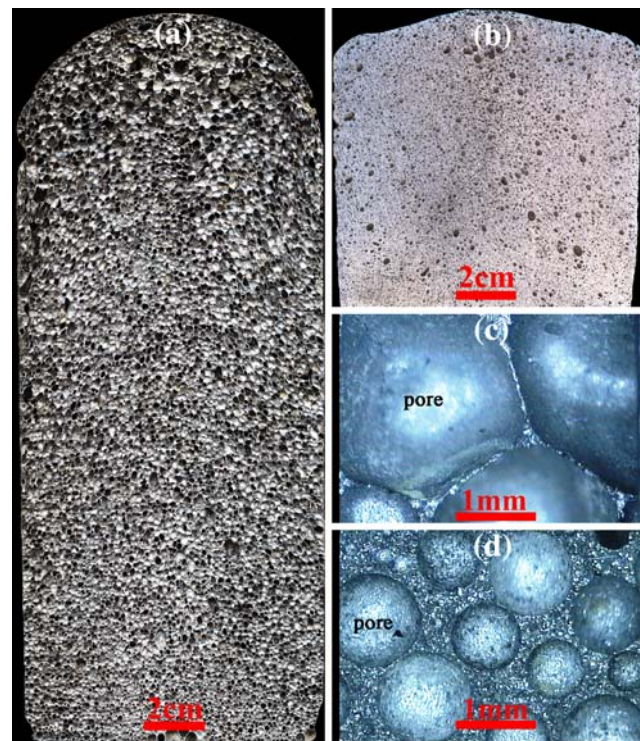
$$Pr = [V_s - (M/\rho)]/V_s \times 100\% \quad (1)$$

where  $\rho$  is the density of the matrix. The quasi-static compression tests were carried out at room temperature on the SS-2202 Universal Testing Machine (Changchun Institute for Testing Machines Co. LTD, China) with a constant cross-head speed of 5 mm/min and the stress ( $\sigma$ )–strain ( $\epsilon$ ) curves were obtained and recorded using a computer.

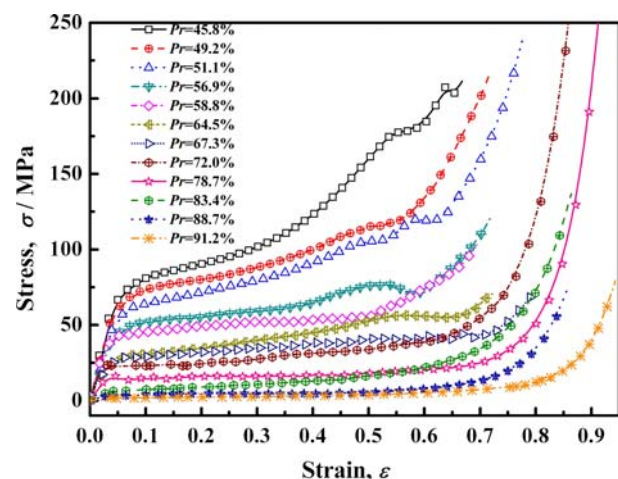
### Results and discussion

Figure 1 demonstrates the section images and corresponding stereo micrographs of cellular AlCu5Mn foams with different pore structures, which shows that both samples have homogenous pore structures and the sample with high porosity (Pr = 86.5%; Fig. 1a) possesses big cell size ( $D > 1$  mm; Fig. 1c), while the sample with low porosity (Pr = 49.0%; Fig. 1b) possesses small cell size ( $D < 1$  mm; Fig. 1d).

Figure 2 is compression stress–strain curves of cellular AlCu5Mn foams with porosities of 91.2–45.8%. Similar to the compression behaviors of other metallic foams, the stress–strain curves of cellular AlCu5Mn foams in Fig. 2



**Fig. 1** Section images and stereo micrographs of cellular AlCu5Mn foam samples. **a** Section image of sample “a” with Pr = 85.6%, **b** section image of sample “b” with Pr = 49.0%, **c** stereo micrograph of the sample “a”, **d** stereo micrograph of the sample “b”



**Fig. 2** Compression stress–strain curves for cellular AlCu5Mn foams with porosities of 45.8–91.2%

consist of three regions, an initial, approximately linear deformation region until the peak stress followed by a softening region to a plateau region, where the stress increases slowly as cells are crushed steadily, and finally the densification region, in which the stress increases rapidly due to the collapsed cells having been almost fully compacted together.

The peak stress is defined as yielding strength,  $\sigma_s^*$ , of a cellular AlCu5Mn foam. The yielding strength values of cellular AlCu5Mn foams as well as those of cellular Al foams [5, 20], cellular Al alloy foams [21–24], porous Al foams [25, 26], porous Al/Al alloy foams prepared in this study, cenosphere-Al syntactic foams [11], Al-steel composite foams [12], and ceramic microballoon reinforced Al matrix composites (microballoon MMCs) [13, 14] are shown in Fig. 3, which indicates that the yielding strength,  $\sigma_s^*$ , of cellular AlCu5Mn foam as well as that of the other Al-based foams has the tendency of decreasing with increasing of porosity, where the  $\sigma_s^*$  of the cellular AlCu5Mn foams with porosity 45.8, 49.2, 51.1, 56.9, 58.8, 64.5, 67.3, 72.0, 78.7, 83.4, 86.3, 88.7, 90.5, and 91.2% are 82.7, 70.3, 63.0, 50.9, 48.3, 43.2, 30.3, 29.0, 24.8, 16.2, 11.3, 6.5, 4.5, and 1.98 MPa, respectively. And at a given porosity, the  $\sigma_s^*$  of the cellular AlCu5Mn foam is higher than all those of the other Al-based foams except those of the Al-steel composite foams and the microballoon MMCs reported in Ref. [12] and Refs. [13, 14], respectively. Notably, a more reasonable comparison about them will be done in the text hereafter.

In particular, the  $\sigma_s^*$  of the cellular Al foams [5, 20] (the red circles in Fig. 3) are comparable with that of the cellular AlCu5Mn foams for a given porosity when Pr is higher than  $\sim 82\%$ , where the  $\sigma_s^*$  of cellular Al foam decreases from 6.2 MPa for porosity of 82.6% to 3.1 MPa for porosity of 90.2%. The  $\sigma_s^*$  of the cellular AlCu5Mn foams are much higher than those of the porous Al foams (the green triangles in Fig. 3) for a given porosity, where the  $\sigma_s^*$  of the porous Al foam decreases from 13.3 MPa for porosity of 51.5% to 0.41 MPa for porosity of 88.3%. The  $\sigma_s^*$  of the cellular AlSi6Cu4 foams prepared by powder

metallurgical method [21] (purple and dark yellow points in Fig. 3) are comparable with those of the cellular AlCu5Mn foams for a given porosity when Pr is higher than  $\sim 79\%$ , where the  $\sigma_s^*$  of the cellular AlSi6Cu4 foam decreases from 21.9 MPa for porosity of 69.7% to 3.6 MPa for porosity of 87.5%. For a given porosity, the  $\sigma_s^*$  of the cellular Al(Si) foams reported in Ref. [5] (orange line in Fig. 3) are in the range of 15.8–28.0 MPa for the porosity range of 77–68%, which are higher than those of the cellular AlSi6Cu4 foams [21], but still lower than those of the cellular AlCu5Mn foams. For a given porosity, the  $\sigma_s^*$  of the porous AlCu5Mn foams with the pore size of 2.0–2.6 mm after T6 heat treatment (pink points in Fig. 3) are higher than those of the other porous Al/Al alloy foams, but still lower than those of the cellular AlCu5Mn foams, where the  $\sigma_s^*$  of the porous AlCu5Mn foam decreases from 50.4 MPa for the porosity of 56.6% to 11.0 MPa for the porosity of 68.7%. Furthermore, according to Fig. 3 (blue points), the values of  $\sigma_s^*$  of the cenosphere-Al syntactic foams with (Pr = 43.7%,  $D = 150 \mu\text{m}$ ) and with (Pr = 40.7%,  $D = 90 \mu\text{m}$ ) are 45 and 75 MPa, respectively [11], which are lower than those of cellular AlCu5Mn foams when their porosities are lower than  $\sim 58$  and  $\sim 47\%$ , respectively.

Figure 3 also demonstrates that the  $\sigma_s^*$  of the Al-steel composite foams (black solid points in Fig. 3) and microballoon MMCs (shaded square in Fig. 3) are higher than those of the cellular AlCu5Mn foams at a given porosity, where the  $\sigma_s^*$  of the composite foams containing low carbon steel (LCS) hollow balls are in the range of 50.7–60.9 MPa for the porosity range of 57.3–58.8%, the  $\sigma_s^*$  of the composite foams containing stainless steel (SS) hollow balls are in the range of 70–90.4 MPa for the porosity

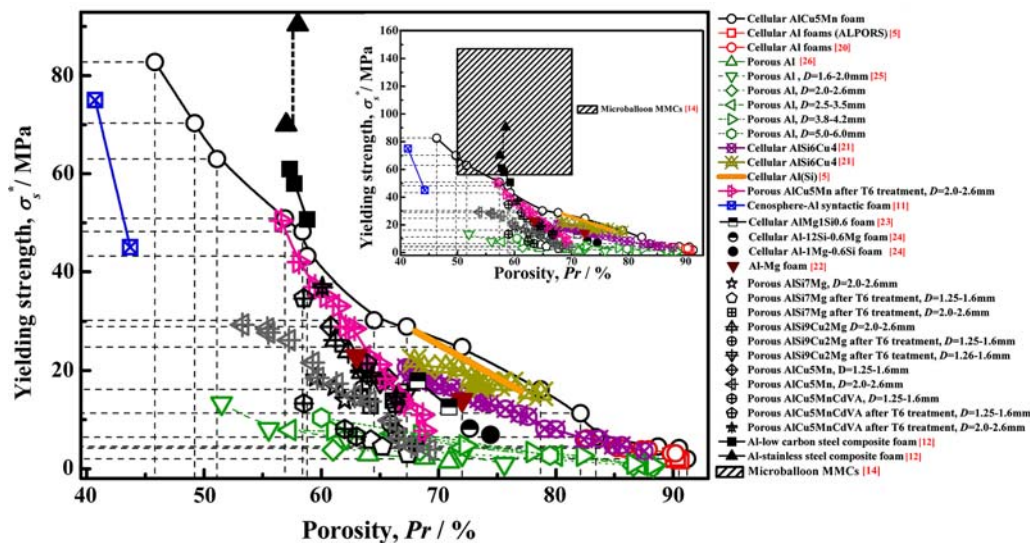


Fig. 3 Relationships between yielding strength and porosity for Al-based foams

range of 57–58% [12] and the  $\sigma_s^*$  of the microballoon MMCs are in the range of 146.9–56.5 MPa for porosity range of 50–70% [14]. The higher strengths of these composite foams are likely attributed to the high volume fraction of LCS/SS hollow sphere (~59 vol.%, 3.7 mm in diameter and 200  $\mu\text{m}$  in wall thickness) or ceramic microballoon (50–70 vol.%, 45 or 270  $\mu\text{m}$  mean diameter) distributed in the Al matrix. On the other hand, the densities of the Al–LCS/Al–SS composite foams and the microballoon MMCs are around  $2.40 \times 10^3 \text{ kg m}^{-3}$  [12] and  $4.2 \times 10^3 \text{ kg m}^{-3}$  [14], respectively, so, the highest specific strengths (yielding strength divided by density) of the Al–LCS/SS composite foam with porosity of 58% and the microballoon MMCs with porosity around 50% are  $37.7 \times 10^3 \text{ m}^2 \text{ s}^{-2}$  and  $35.0 \times 10^3 \text{ m}^2 \text{ s}^{-2}$ , respectively, which are both lower than the specific strength of the cellular AlCu5Mn foams ( $41.7 \times 10^3 \text{ m}^2 \text{ s}^{-2}$ ) for the porosity lower than 58.4%.

The energy absorption capacity ( $C$ ) of the cellular AlCu5Mn foams is calculated as the area under the stress–strain curves shown in Fig. 1 by using Eq. 2 and the results are shown in Fig. 4, which indicates that the  $C$  value of the cellular AlCu5Mn foam increases when the porosity decreases at a given strain.

$$C = \int_0^\varepsilon \sigma \cdot d\varepsilon, \tag{2}$$

In particular, in Fig. 4, the solid black squares on the  $C$ – $\varepsilon$  curves represent the positions indicating the energy absorption capacity at 0.5 strain ( $C_{0.5}$ ) for cellular AlCu5Mn

foams, where the value of  $C_{0.5}$  increases from  $1.3 \text{ MJ m}^{-3}$  (for porosity of 91.2%) to  $49.3 \text{ MJ m}^{-3}$  (for porosity of 45.8%). The relationship between  $C_{0.5}$  values of the cellular AlCu5Mn foams and porosity are shown in the left top small figure in Fig. 4. For porosities lower than 47.6% (point A in Fig. 4), the  $C_{0.5}$  values of the cellular AlCu5Mn foams will be larger than  $44 \text{ MJ m}^{-3}$ , which is higher than those of the Al–steel composite foams ( $24.4$ – $44 \text{ MJ m}^{-3}$  for the porosity of ~58% [12]).

According to the data in Figs. 2 and 4, the  $C$  values of the cellular AlCu5Mn foams at the densification strain ( $C_d$ ) can be determined by the  $C$ – $\sigma$  curves shown in Fig. 5, where the solid black circles represent the positions indicating the  $C_d$  values. Figure 5 shows that the  $C_d$  values possess the tendency of increasing with decreasing of porosity, where the  $C_d$  value of the cellular AlCu5Mn foam increases from  $2.70 \text{ MJ m}^{-3}$  (for porosity of 91.2%) to  $72.22 \text{ MJ m}^{-3}$  (for porosity of 45.8%).

Specifically, according to the experimental  $C_d$  and Pr values, a relationship between  $C_d$  and Pr can be obtained (see the left top small figure in Fig. 5), which indicates that for the porosities lower than ~75% (point A in Fig. 5), the  $C_d$  values of the cellular AlCu5Mn foams will be higher than  $13 \text{ MJ m}^{-3}$ , which is higher than those of Al alloy foams reported in Ref. [6]; for the porosities lower than 66.0% (point B in Fig. 5), the  $C_d$  values of the cellular AlCu5Mn foams will be larger than  $20 \text{ MJ m}^{-3}$ , which are higher than those of cenosphere–Al syntactic foams with porosity of 43.7% ( $C_d$  is ~ $20 \text{ MJ m}^{-3}$ ) [11] and for the porosities lower than 56.5% (point C in Fig. 5), the  $C_d$  values of the cellular AlCu5Mn foams will be larger than

**Fig. 4** Relationships between energy absorption capacity and strain for cellular AlCu5Mn foams with porosities of 45.8–91.2%. The small figure on the left top shows the relationship between energy absorption capacity at 0.5 strain,  $C_{0.5}$ , and porosity, Pr, for cellular AlCu5Mn foams

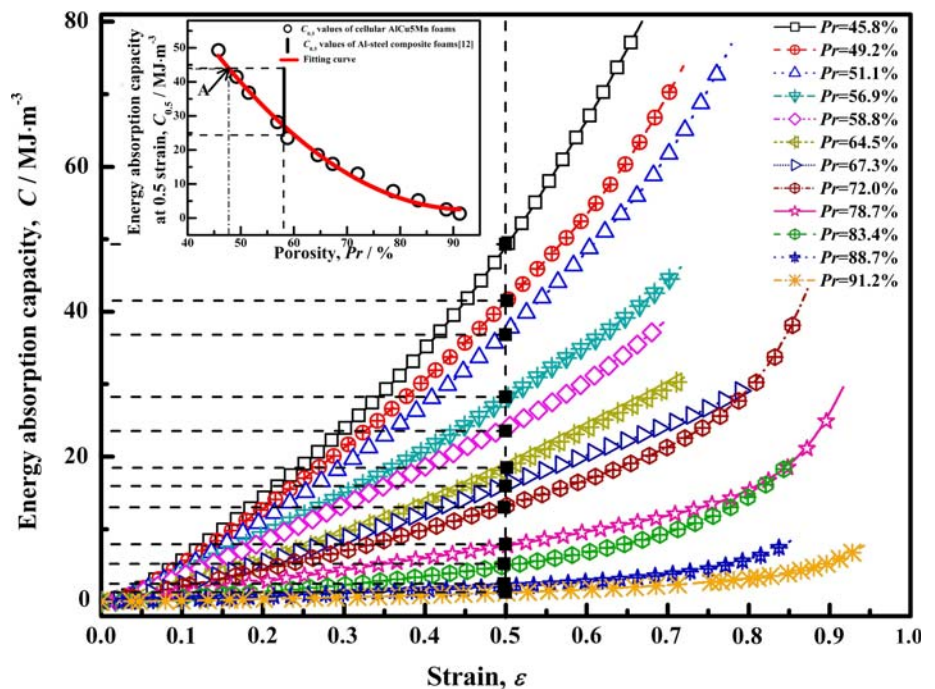
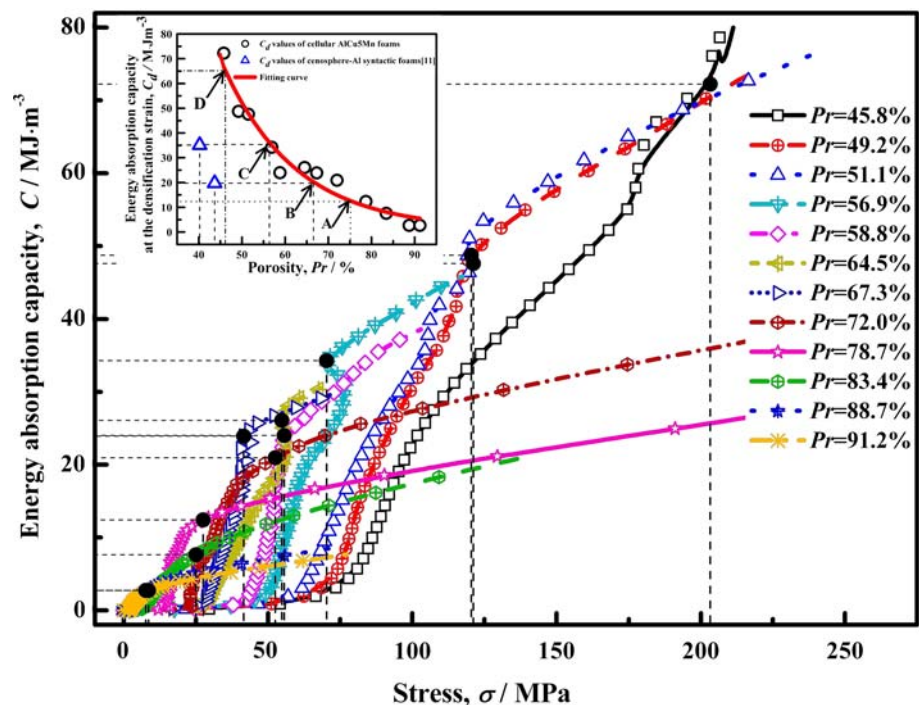


**Fig. 5** Relationships between energy absorption capacity and stress for cellular AlCu5Mn foams with porosities of 45.8–91.2%. The small figure on the left top shows the relationship between energy absorption capacity at densification strain,  $C_d$ , and porosity, Pr, for cellular AlCu5Mn foams



$35 \text{ MJ m}^{-3}$ , which are higher than those of cenosphere-Al syntactic foams with porosity of 40.7% ( $C_d$  is  $\sim 35 \text{ MJ m}^{-3}$ ) [11]; for the porosities lower than  $\sim 46\%$  (point D in Fig. 5), the corresponding  $C_d$  values of the cellular AlCu5Mn foams will be higher than  $65 \text{ MJ m}^{-3}$ , which is higher than the maximum  $C_d$  value of the microballoon MMCs ( $\approx 65 \text{ MJ m}^{-3}$ ) [13].

## Conclusion

In summary, for cellular AlCu5Mn foams prepared by melt foaming method, there exist relationships among the porosity, the strength, and the energy absorption capacity: for the porosity decreasing from 91.2 to 45.8%, the corresponding strength increasing from 1.98 to 82.7 MPa and the energy absorption capacity increasing from 2.70 to  $72.22 \text{ MJ m}^{-3}$ , which makes this material a promising future in the applications requiring any pair of values of strength and energy absorption capacity in the wide range.

**Acknowledgements** This work is supported by the Research Fund for the Doctoral Program of Higher Education of China (Grant. No. 200802941010), the Natural Science Foundation of HoHai University (Grant. No. 2008428011) and Scientific Research Startup Fund of HoHai University (Grant No. 2084140801109).

## References

1. Degischer HP, Kriszt B (2005) Handbook of cellular metals. Wiley-VCH, Chemical Industry Press, pp 150–270 (trans: Zuo XQ, Zhou Y)

2. Banhart J (2002) Prog Mater Sci 46:559
3. Banhart J (2005) Int J Veh Des 37:114
4. Dannemann KA, Lankford J Jr (2000) Mater Sci Eng A 293:157
5. Mukai T, Kanahashi H, Miyoshi T, Mabuchi M, Nieh TG, Higashi K (1999) Scripta Mater 40:921
6. Simone AE, Gibson LJ (1998) Acta Materilia 46:3109
7. Thornton PH, Magee CL (1975) Metall Trans 6B:1253
8. Yang DH, He DP, Yang SR (2004) Sci China B 47(6):512
9. Yang DH, Hur BY (2006) Mater Lett 60:3635
10. Yang DH, Hur BY, He DP, Yang SR (2007) Mater Sci Eng A 445–446:415
11. Wu GH, Dou ZY, Sun DL, Jiang LT, Ding BS, He BF (2007) Scripta Mater 56:221
12. Vendra LJ, Rabiei A (2007) Mater Sci Eng A 465:59
13. Kiser M, He MY, Zok FW (1999) Acta Mater 47:2685
14. Palmer RA, Gao K, Doan TM, Green L, Cavallaro G (2007) Mater Sci Eng A 464:85
15. Kaufan JG, Rooy EL (2004) Aluminum alloy castings: properties, process and applications. ASM International, Materials Park, p 13
16. An JR, Tian LG (2008) Handbook of metal materials. Chemical Industry Press, Beijing, p 508
17. Yang DH, He DP (2001) Sci China B 44(4):411
18. Chen C, Wang YJ, He DP (2003) Chin J Mater Res 17(3):230
19. Ashby MF, Evans AG, Fleck NA, Gibson LJ, Hutchinson JW, Wadley HNG (2000) Metal foam: a design guide. Butterworth-Heinemann Press, Boston, p 26
20. Wu ZJ, He DP (2001) J Appl Sci 19(4):357
21. Banhart J, Baumeister J (1998) J Mater Sci 33:1431. doi: 10.1023/A:1004383222228
22. Kitazono K, Kikuchi Y, Sato E, Kuribayashi K (2007) Mater Lett 61:1771
23. McCullough KYG, Fleck NA, Ashby MF (1999) Acta Mater 47(8):2323
24. Markaki AE, Clyne TW (2001) Acta Mater 49:1677
25. Jiang B, Wang ZJ, Zhao NQ (2007) Scripta Mater 56:169
26. Han FS, Cheng HF, Wang JX, Wang Q (2004) Scripta Mater 50:13